Chemistry & Biodiversity

WILEY-VCH

CHEMISTRY & BIODIVERSITY

RESEARCH ARTICLE

Green Synthesis of Zinc Oxide Nanoparticles Including Rosehip (*Rosa canina* L.) Seed Extract: Evaluation of Its Characterization and Bioactivity Properties

Rabia Nur Bozkurt[1,2] | Selin Şahin[1]

[1]Chemical Engineering Department, Istanbul University-Cerrahpasa, Istanbul, Turkey | [2]Faculty of Engineering and Natural Sciences, Chemical Engineering Department, Istanbul Health and Technology University, Istanbul, Turkey

Correspondence: Rabia Nur Bozkurt (rabia.bozkurt@istun.edu.tr)

Received: 23 October 2024 | **Revised:** 19 December 2024 | **Accepted:** 24 December 2024

Funding: The authors received no specific funding for this work.

Keywords: antioxidant activity | green synthesis | nanoparticles | rosehip seed

ABSTRACT

The use of bioactive compounds in plants as reducing, stabilizing, and capping agents in nanoparticle manufacturing is an exceptionally eco-friendly approach. This work used rosehip seed extract, acquired by automatic solvent extraction, in the microwave-assisted green production of zinc oxide nanoparticles (ZnO NPs). The total phenolic content (TPC), total flavonoid content (TFC), and antioxidant activity of the extracted materials and nanoparticles (NPs) were assessed using the 2,2-diphenyl-1-picrylhydrazyl (DPPH) and 2,2′-azinobis(3-ethylbenzothiazoline-6-sulfonic acid) (ABTS) assays. The ideal synthesis parameters were established as 25 mL of extract, pH 12, 360 W of microwave power, and a metal salt concentration of 0.05 M for a duration of 7 min. The characterization of the ZnO NPs synthesized under these conditions was performed using x-ray diffraction (XRD), Fourier-transform infrared spectroscopy (FT-IR), scanning electron microscopy with energy-dispersive x-ray analysis (SEM-EDX), dynamic light scattering (DLS), zeta potential measurements, and UV–Vis spectrophotometry. High-purity, nano-sized, antioxidant ZnO NPs were manufactured using an ecologically friendly, sustainable, and ecological technique.

1 | Introduction

The idea of nanotechnology was popularized in the 1960s by Richard Feynman, whereas earlier scientists had used minuscule materials without knowledge [1]. The discipline of nanotechnology is progressing by the synthesis of nanomaterials with controlled dimensions [2]. Nanoparticles (NPs) are often defined as particles that measure 100 nm or smaller in at least one dimension. It is essential to note that NPs exhibit distinct and frequently enhanced physico-chemical properties relative to the corresponding bulk material [3]. The chemical and physical properties of nanoscale materials are affected by their surface atoms, as a higher surface-to-volume ratio reduces grain size and decreases the melting point of surface atoms, hence influencing their chemical and physical characteristics [4]. Due to the reliance of nanotechnology on the utilization of materials and gadgets via nanoscale techniques across many fields, NPs have emerged as a prominent substance for the advancement of science and technology in recent years [5]. Nanoscience has swiftly advanced owing to its prospective uses across diverse industries and has emerged as a significant aspect of everyday life [6]. Nanomaterials have many applications in medical, cosmetics, packaging, nanofibers, biosensors, and electronics, now attracting significant interest owing to their magnetic, catalytic, mechanical, optical, and electrical properties [7, 8]. A diverse array of metal-based NPs has been precisely synthesized, including gold, silver, aluminum,

copper, magnesium, palladium, zinc, and platinum [6, 9–13]. Metal oxide NPs may be manufactured by connecting two metal segments (–O–) with oxy or hydroxyl bridges (–OH–), leading to the creation of metal oxide or metal hydroxide NPs in an aqueous solution [14]. Zinc oxide nanoparticles (ZnO NPs) have attracted significant interest across several industries, including optics, electronics, packaged foods, and medicine, due to their advantageous properties such as biocompatibility, minimal cytotoxicity, and cost-effectiveness [15–18]. A ZnO semiconductor, characterized by a band gap energy of around 3.37 eV, has many uses in photocatalysis, sensing, optoelectronics, and biomedical sciences [2, 18, 19]. ZnO has considerable economic and industrial significance due to its varied properties, facilitating its employment in several industries, such as the rubber industry, biomedical fields, and metal surface treatment [20]. In recent years, there has been an increasing emphasis on the creation of ecologically sustainable goods and processes, driven by concerns over climate change, water pollution, finite natural resources, and human health. In several fields, NPs have emerged as a prominent material for the advancement of science and technology in recent years [20–22]. Top–down and bottom–up approaches form the basis of different methodologies for NP synthesis. The top–down technique involves reducing the bulk material to tiny NPs by breaking it into its monomers, whereas the bottom–up synthesis constructs NPs from atoms. The synthesis of NPs employs a variety of chemical, physical, and, more recently, biological methods [3, 23]. The advancement and requirement of green synthesis techniques to produce NPs have attracted significant popularity in recent years.

Green synthesis denotes the ecologically sustainable creation of various nanomaterials [24]. Physical and chemical synthesis procedures are often expensive, require the use of hazardous chemicals and specialized equipment, and are detrimental to the surrounding environment. Thus, green synthesis is an environmentally sustainable and cost-effective approach [2]. Diverse compounds such as proteins, alkaloids, flavonoids, reducing sugars, and polyphenols in biomaterials serve as reducing and capping agents in the synthesis of NPs from metal salt precursors [25]. The availability of phytochemicals in plant extracts, which function as stabilizing and reducing agents, has resulted in the use of diverse plant components—such as leaves, fruits, roots, stems, and seeds—for the synthesis of different NPs [26]. The ecologically sustainable production of ZnO NPs by plant extract encompasses a three-phase process: reduction, nucleation, and stabilization [27]. The extract's bioactive components, including flavonoids, phenolic acids, and tannins, are essential in promoting the process. The phytochemicals in the aqueous extract reduce zinc ions from the zinc precursor, such as zinc nitrate. This reaction results in the creation of zinc hydroxide, as shown in Equation (1). Under various conditions, such as heat treatment or pH alteration, the reaction decomposes, producing ZnO and releasing water, as demonstrated in Equation (2). Phytochemicals encapsulate and stabilize the synthesized ZnO NPs, preventing their agglomeration. The phytochemical coating not only improves the stability of the NPs but also imparts potential bioactive capabilities (Equation 3) [27, 20]:

$$Zn^{2+} + \text{phytochemicals} \rightarrow Zn(OH_2) \downarrow \quad (1)$$

$$Zn(OH_2) \xrightarrow{\text{heat or pH adjustment}} ZnO + H_2O \quad (2)$$

$$ZnO + \text{phytochemicals (Stabilizers)} \rightarrow \text{stabilized ZnO NPs} \quad (3)$$

The production of ZnO NPs using plant extracts as support has been examined in earlier research. Ifeanyichukwu et al. [28] successfully produced ZnO NPs by green synthesis employing aqueous extracts from pomegranate (*Punica granatum*) leaves and flowers. Alharthi et al. [29] synthesized ZnO NPs by a simple and modern technique employing aqueous *Ziziphus jujuba* leaf extract, aided by microwave irradiation. Jamdagni et al. [30] documented an ecologically sustainable method for synthesizing ZnO NPs using the aqueous flower extract of *Nyctanthes arbortristis*. MuthuKathija et al. [31] used reducing and capping agents from *Pisonia alba* leaf extract for the eco-friendly production of ZnO NPs. Du et al. [32] used *Sida acuta* leaf extract in their research as a capping and reducing agent that encouraged nucleation and morphological development.

The genus *Rosa*, under the Rosaceae family, has over 100 species distributed over Europe, Asia, and North America, with its medicinal and nutritional advantages acknowledged and used for thousands of years [33]. *Rosa canina* L. is a member of the Rosaceae family, recognized for its white flowers and luminous red rosehips [34]. Due to its high concentrations of various bioactive compounds with antioxidant properties, such as vitamin C, carotenoids, and known as "rosehip" is known for its therapeutic properties in treating hemorrhoids and diabetes mellitus, as well as its anti-inflammatory and anti-obesity effects [35–37]. Often, people do not eat the fruits fresh; instead, they use them to make marmalade, jams, juices, teas, syrups, wine, and more recently, probiotic beverages, yogurts, and soups [38]. Every year, people discard several rosehip seeds, despite the seed making up a substantial portion of the fruit. In this context, seeds are classified as substantial agricultural and industrial waste [39]. Advanced extraction techniques enhance efficiency and selectivity, while reducing processing time and expenses. Additionally, this method minimizes solvent use, substitutes conventional solvents with more eco-friendly and safer alternatives, and ensures the safety of the final extract [40]. Automatic solvent extraction (ASE) is a solid–liquid extraction technique conducted at elevated temperatures (50°C–200°C) and high pressures (10–15 MPa), with its primary benefits over conventional extraction techniques being significant reductions in solvent use and extraction duration [41]. Furthermore, ASE has shown promising results in the extraction of bioactive compounds, especially with green solvents [42]. Ethanol is used for its cost-effectiveness and in scenarios where the objective is to get moderately polar compounds, such as phenolic acids [43]. This study used rosehip seeds, a significant element of the fruit, for the first green synthesis of ZnO NPs. ASE, a novel method for extracting plant material, decreased both extraction duration and solvent use. The extract's and ZnO NPs's total phenolic content (TPC), total flavonoid content (TFC), and antioxidant activity were assessed using spectrophotometric methods. The synthesis of ZnO NPs was conducted in a sustainable and environmentally benign way using a polyphenol-rich extract derived from seeds that would otherwise be considered waste. ZnO NPs were produced with a microwave heating method, leading to enhanced time efficiency. The synthesis of ZnO NPs was optimized using a UV–Vis spectrophotometer to determine the optimum synthesis parameters. The synthesized ZnO NPs were examined using x-ray diffraction (XRD), Fourier transform infrared spectroscopy

(FT-IR), scanning electron microscopy with energy dispersive x-ray analysis (SEM-EDX), dynamic light scattering (DLS), zeta potential assessments, and UV–Vis spectrophotometry. We anticipate that the eco-friendly method of synthesizing pure and nano-sized ZnO NPs will illuminate future research.

2 | Materials and Methods

2.1 | Materials

2.1.1 | Plant Materials

The fresh rosehip (*R. canina* L.) fruit samples used in this research were collected by Rabia Nur Bozkurt from Çerkeş, Çankırı, Turkey (Central Anatolia Region; latitude 40° 48′ N, longitude 32° 53′ E, height 800 m) in September 2023. The seeds of some harvested fruits were collected, whereas the fruit was still fresh. The seeds of some harvested fruits were extracted, whereas the fruit remained fresh. A portion of the fruit was desiccated by sunlight. The seeds of dried rosehip fruit were extracted. A part of the fresh fruit was converted into marmalade. The fruits were cooked, strained through a sieve, leaving the seeds behind. Distilled water was used to cleanse the beans adhering to the strainer. The seeds left after the fruit was processed into marmalade constituted the predominant portion of the plant material. The core, acquired under three distinct conditions, was preserved in the refrigerator at −25°C until the extraction phase.

2.1.2 | Chemical Materials

Ethanol (≥99.9%) (EtOH) was obtained from Merck (Darmstadt, Germany) for the extraction process. Sodium carbonate (≥99.0%) (Na_2CO_3), sodium hydroxide (NaOH), (+)-catechin, 2,2-diphenyl-1-picrylhydrazyl (DPPH), 2,2′-azinobis(3-ethylbenzothiazoline-6-sulfonic acid) (ABTS), 6-hydroxy-2,5,7,8-tetramethylchroman-2-carboxylic acid (Trolox), butylated hydroxytoluene (BHT), Folin–Ciocalteu reagent, and gallic acid monohydrate (≥98.0%) were procured from Sigma-Aldrich (St. Louis, MO, USA). Methanol (≥99.9%) (MeOH) was obtained from Merck (Darmstadt, Germany). Zinc nitrate hexahydrate ($Zn(NO_3)_2{\cdot}6H_2O$) utilized for NP manufacturing was procured from Merck (Darmstadt, Germany). Deionized water was provided by the Millipore Milli-Q purification system.

2.2 | Methods

2.2.1 | Rosehip Seed Extract Preparation

An environmentally friendly method, specifically ASE technology, was utilized to extract a phytochemically rich material from rosehip seeds. The rosehip (*R. canina* L.) seeds, stored at −25°C, were prepared for extraction by air-drying at room temperature and washing twice with pure water.

2.2.2 | Automatic Solvent Extraction

Extraction of rosehip seeds was carried out with an automatic solvent extractor (Velp Scientifica, Usmate, Italy). Rosehip seed samples (1 g) were placed in extraction cartridges (Whatman, Maidstone, UK, 33 mm × 80 mm). Then, 80 mL of extraction solvent was added to the extraction containers. Depending on the type of solvent, extraction temperature, washing time, immersion time, removal time, and recovery time are set on the device screen. A period of 20 min for immersion, 40 min for washing, 30 min for recovery, and 2 min for cooling were adjusted to the appropriate temperature level according to the solvent type. Extraction time lasted 1 h 32 min. The extract was filtered using a 0.45 μm syringe filter. The extract was stored in an amber bottle at +4°C [42].

2.3 | Quantitative Determination of Phytochemical Constituents

2.3.1 | Determination of TPC

The Folin–Ciocalteu technique was used to quantify the TPC of rosehip seed extract and ZnO NPs. The same procedure was applied for both. A volume of 20 μL of the sample was taken, and 380 μL of distilled water was added. Subsequently, 2000 μL of Folin–Ciocalteu reagent and 1600 μL of sodium carbonate solution were included. Absorbance measurements were recorded at 765 nm using a UV spectrophotometer (PG Instruments, T60, Leicestershire, UK), with samples stored in darkness for 30 min. Calibration curves were determined using suitable solvents obtained from pure gallic acid, with results expressed as milligrams of gallic acid equivalent per gram of dry matter (mg GAE/g DM) [44].

2.3.2 | Determination of TFC

The aluminum chloride method was used to measure the TFC of rosehip seed extract and ZnO NPs. The same approach was utilized for both. A 25 μL sample was taken, and then 2225 μL of distilled water was added. Subsequently, 113 μL of $NaNO_2$ was introduced and maintained in darkness for 6 min. A volume of 225 μL of $AlCl_3$ was incorporated into the mixture and allowed to stand for 5 min in darkness. Ultimately, 750 μL of NaOH and 412 μL of distilled water were included, respectively. Absorbance measurements were obtained using a UV spectrophotometer (PG Instruments, T60/Leicestershire, England) at a wavelength of 510 nm. Calibration curves were established with catechin as a reference standard. Results are presented as milligrams of catechin per gram of dry matter (mg CE/g DM) [45].

2.3.3 | Determination of Antioxidant Activity by DPPH Method

The antioxidant activity of the extract and NP solution was evaluated using the DPPH method. The same technique was used for each. A solution was made by diluting 0.0079 g of DPPH in 40 mL of methanol (80% v/v). After that, 600 μL of methanol (80% v/v) and 3000 μL of diluted DPPH solution were added to 100 μL of the sample solution. The mixture was then left alone for 30 min in the dark. The antioxidant activity was quantified spectrophotometrically at 517 nm by the DPPH technique. BHT was used as the control. Calibration curves were developed using Trolox (6-hydroxy-2,5,7,8-tetramethylchroman-2-carboxylic acid)

in suitable solvents. The outcomes were quantified as milligrams of Trolox equivalent antioxidant activity (mg TEAC/g DM) per gram of dry matter [46]. The ability to scavenge the DPPH radical was determined using the following equation:

$$\text{Antioxidant activity (\%inhibition)} : \frac{A_{\text{control}-}A_{\text{sample}}}{A_{\text{control}}} \times 100 \quad (4)$$

where A_{control} is the absorbance of the control (DPPH solution without sample), and A_{sample} is the absorbance of the test sample.

2.3.4 | Determination of Antioxidant Activity by ABTS Method

The free radical scavenging activity of the extract and NPs was evaluated using the ABTS assay. The same approach was implemented for both. Following the addition of 150 µL of sample solution to 2850 µL of diluted ABTS solution, absorbance was recorded at the 10th minute at 734 nm, using a blank sample empty of ABTS as a reference. BHT was used as the control. Results were presented as milligrams of trolox equivalent antioxidant capacity per gram of dry matter (mg TEAC/g DM) [47]. Scavenging activity of the samples against the ABTS radical was stated as written in Equation (4).

2.4 | ZnO NPs Synthesis

The synthesis conditions for ZnO NPs from rosehip seed extract were adjusted by changing many parameters using a UV–Vis spectrophotometer. Following the establishment of optimal synthesis conditions, a 0.5 M solution of 50 mL $Zn(NO_3)_2{\cdot}6H_2O$ was produced. A volume of 25 mL of the rosehip seed extract was thereafter added dropwise to the metal precursor while being stirred on a magnetic stirrer. The pH of the synthesis was adjusted to 12 with 1 M NaOH. The procedure continued for 7 min under microwave irradiation at 360 W. The procedure was conducted in a microwave extraction reactor (NEOSGR, Milestone Srl, Italy). The resultant milky ZnO NPs suspension underwent centrifugation at 4000 rpm for 15 min. The supernatant was discarded, and the precipitate was washed with ethanol and filtered water to eliminate any remaining contaminants. The precipitate was then dried in an oven at 80°C for 24 h. Upon drying, the precipitate was ground in a mortar and preserved in Eppendorf tubes at +4°C for further characterization and spectrophotometric analysis.

2.5 | ZnO NPs Characterization

The characterization of ZnO NPs synthesized using the green method was performed through absorbance measurements to optimize various parameters on a UV–Vis spectrophotometer (Agilent/8453, Victoria, Australia). The samples were diluted with distilled water, placed in quartz cuvettes, and measurements were conducted within the wavelength range of 300–500 nm. UV–Vis diffuse reflectance spectra (DRS) were obtained using the (PG Instruments T92+, Leicestershire, UK) spectrophotometer across a wavelength range of 300–600 nm. An XRD machine (Rigaku/R-Axis Rapid-S, Tokyo, Japan) was used to study the structure of crystalline NPs. Data were collected at a step size of 0.01 across the range of $2\theta = 10°–80°$. FT-IR (Bruker/Tensor 27, MA, USA) was used to identify the functional groups of the synthesized ZnO NPs. Measurements were conducted within the range of 400–4000 cm^{-1}. The surface shape and elemental content of the produced NPs were examined using scanning electron microscopy (SEM) (Zeiss Evo LS 10, Jena, Germany). DLS using a Brookhaven 90 Plus Nano Particle Size Analyzer (New York, USA) assessed the average size, size distribution, and polydispersity index (PDI) of the NPs. Finally, the effective electrical charge on the surface of the synthesized ZnO NPs was determined using the Zetasizer (Malvern Nano ZS, Malvern, UK).

2.6 | Statistical Analysis

Analysis of variance test (ANOVA) was used to measure the significance between the groups for the findings of bioactivity tests. Therefore, InStat software (GraphPad, San Diego, CA, USA) was used to analyze the means of three replicate ($n = 3$) results via Tukey's test.

3 | Results and Discussions

3.1 | Determination of Phytochemical Content of Plant Extract

Given the recognized significance of phenolic compounds in plant extracts as reducing, stabilizing, and capping agents in the development of metallic NPs [48], we assessed the three varieties of discarded rosehip seeds for their TPC to determine the most suitable seed type. The optimal solvent type and concentration for TPC were assessed, and the extract was prepared using the suitable solvent type and concentration. The extracted material was assessed for TFC, TPC, and antioxidant activity using the DPPH and ABTS assays and was used in the synthesis of ZnO NPs. ASE subjected three varieties of rosehip seed samples—seeds extracted from fresh fruit (S1), seeds extracted from dried fruit (S2), and seeds extracted after thermal treatment of the fruit (S3)—to extraction using an 80% ethanol solution. Figure 1a indicates that S1 exhibits the lowest TPC, but S2 has a greater TPM compared to S1. S3 achieved the maximum TPC. This scenario is believed to be associated with the rupture of the cell wall in the rosehip seed tissue prior to extraction, influenced by temperature and vapor pressure, resulting in an increase in the release of phenolic compounds from the cell walls. The predominance of seed debris derived from the thermal processing of the fruit indicates its advantageous role in trash recycling within the study's framework. Once the core type with the highest TPC was identified, the process of selecting the most suitable solvent commenced. Numerous factors, including plant composition, extraction method, solvent type, and plant-to-solvent ratio, affect the extraction of biologically active compounds from plants. The solvent is a critical variable when the extraction time and temperature are held constant. The use of ethanol or an aqueous ethanol solution, both polar solvents, during the extraction process promotes a more ecologically friendly method for using the extract in food and health applications [49]. Rosehip seeds were extracted using distilled water and ethanol solutions of varying strengths, and their TPC was analyzed. Figure 1b illustrates that the lowest TPC was determined during the extraction

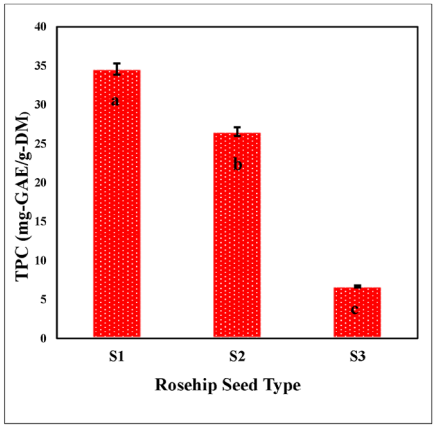

(a)

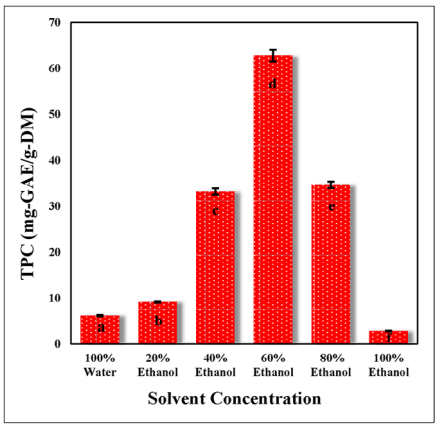

(b)

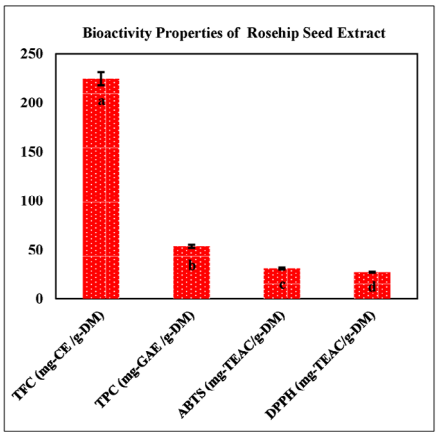

(c)

FIGURE 1 | (a) Determination of TPC in several rosehip types, (b) determination of TPC in different solvent concentration, (c) bioactivity properties of plant extract. The data are presented as the mean ($n = 3$) ± standard deviation. Different letters within each column indicate significant differences between treatments according to Tukey's test at $p < 0.001$. ABTS, 2,2′-azinobis(3-ethylbenzothiazoline-6-sulfonic acid); DPPH, 2,2-diphenyl-1-picrylhydrazyl; TFC, total flavonoid content; TPC, total phenolic content.

with pure water and 100% ethanol. Prior research has shown that alcohol–water combinations outperform single-component solvents in the extraction of phenolic compounds [49–51]. Water acts as a swelling agent for cells, enhancing the contact surface between the plant matrix and the solvent; therefore, it raises the concentration of phenolic compounds. TPC increased with rising ethanol concentration up to 60%, after which it started to decrease. This occurs because when the concentration of ethanol is above a certain threshold, it denatures proteins, inhibiting the dissolution of polyphenols and reducing the TPM value [52]. Figure 1c displays the TPC, TFC, and antioxidant activity values of rosehip seed extract. The TPC of rosehip seed extract was measured as 53.62 ± 0.012 mg GAE/g DM. İlyasoğlu's work on the characterization of rosehip seed and seed oil revealed that the concentration of phenolic compounds in rosehip seed extract was lower than that observed in our research [36]. Our research obtained results similar to the phenolic chemicals generated by Demir et al. from rosehip fruit [53]. Variations in factors like the plant's genotype, cultivation location, extraction process, and solvent used influence the TPC, resulting in disparate findings among research [54]. The TFC value of rosehip seeds was determined to be 224.42 ± 0.002 mg CE/g DM. The TFC value of rosehip seed extract was determined to be greater than the flavonoid content reported by Paunović et al. in their investigation of rosehip fruit [35]. This variance is believed to result from variations in the extraction process and solvent conditions used. Changes in plant species also contribute to these differences. The DPPH technique determined the antioxidant activity to be 27.23 ± 0.002 mg TEAC/g DM, whereas ABTS assays gave 31.14 ± 0.002 mg TEAC/g DM. ABTS finding is higher than that of DPPH. This is in agreement with the report of Gaber et al. on pomegranate residue extracts [55]. They recommended ABTS assay as a more sensitive method and better choice comparing to DPPH assay. The scavenging activity of the rosehip seed extract against DPPH radicals was determined to be 97%, demonstrating a remarkable antioxidant capacity. In comparison, the positive control, BHT, exhibited a scavenging activity of 89%. Similarly, when evaluated using the ABTS radical scavenging assay, the extract showed an even higher activity of 98%, whereas BHT demonstrated a scavenging activity of 92%. In both tests, these results show that rosehip seed extract is better at getting rid of radicals than the standard antioxidant, BHT. To conclude, the three groups show significant difference in terms of bioactive properties at $p < 0.001$.

3.2 | Optimization of ZnO NPs Synthesis Conditions

Prior research indicated that concentration, temperature, NP size and morphology, pH, and other factors influenced surface plasmon resonance (SPR) bands. Several elements influence it, as evidenced by previous research [56]. Consequently, an initial metal salt concentration, extract amount, pH, microwave power, and microwave duration were optimized for the production of ZnO NPs. Given that ZnO exhibits significant optical absorption in the 315–400 nm range, conditions were adjusted by conducting absorbance measurements over the 300–500 nm wavelength spectrum using a UV–Vis spectrophotometer.

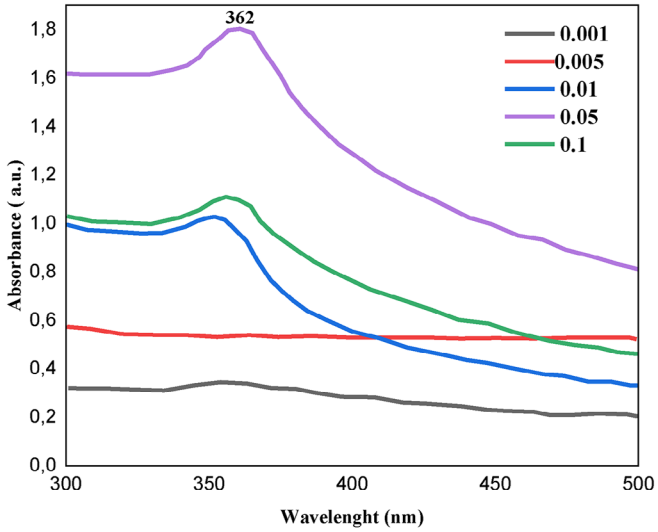

FIGURE 2 | Determination of optimum initial metal salt concentration.

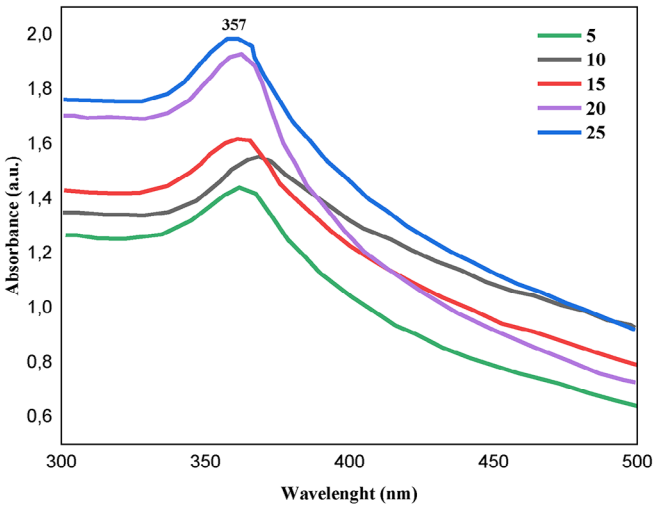

FIGURE 3 | Determination of optimum extract amount.

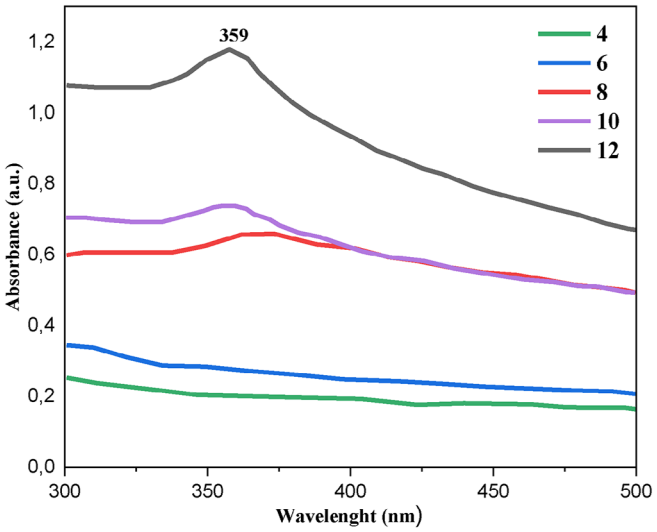

FIGURE 4 | Determination of optimum pH value.

3.2.1 | Determination of Optimum Initial Metal Salt Concentration

The initial metal salt concentration was adjusted for the production of ZnO NPs. To get the best results, 50 mL solutions of $Zn(NO_3)_2{\cdot}6H_2O$ were used at concentrations of 0.001, 0.005, 0.01, 0.05, and 0.10 M. The extract, pH, microwave power, and microwave duration were all kept the same. UV–Vis spectrophotometry used a wavelength range of 300–500 nm. Figure 2 displays the results of absorbance measurements conducted within the specified range. At low concentrations, no analytical signal was found. However, strong absorbance values were recorded at 0.01, 0.05, and 0.10 M. The highest absorbance was found at 0.05 M $Zn(NO_2)_2{\cdot}6H_2O$, after ground adjustments were made. The peak wavelength reported was 362 nm. When the initial metal salt concentration exceeds a certain point, it halts the reduction of metal ions, resulting in the formation of fewer ZnO NPs. Moreover, prior studies indicate that a rise in metal salt concentration leads to bigger particle sizes owing to the heightened presence of metal ions, resulting in the agglomeration of NPs [57]. Consequently, an increase in metal salt concentration from 0.05 to 0.10 M resulted in a reduction in absorption. The extract's biomolecules may not be able to turn metal ions into NPs as metal ions increase. This could potentially lead to a decrease in the formation of ZnO NPs [58].

3.2.2 | Determination of Optimum Extract Amount

Second, the extraction quantity was modified for the production of ZnO NPs. To optimize the conditions, the concentrations of metal salts, pH, microwave power, and microwave duration were held constant, whereas the extract volumes were varied at 5, 10, 15, 20, and 25 mL. Figure 3 presents absorbance data acquired from the UV–Vis spectrophotometer in the 300–500 nm wavelength spectrum. An analytical signal was identified within the typical wavelength range for all extract amounts, with absorbance values increasing in direct correlation to the extract quantity. The maximum absorbance value, after background corrections, was recorded at 357 nm with the application of 25 mL of extract. The bioactive compounds in the extract serve as reducing agents, resulting in elevated absorbance values with increasing extract quantity, hence enhancing the concentration of ZnO NPs. Notwithstanding the noted rise in absorbance within the standard wavelength range of ZnO, even with diminished extract amounts, it is postulated that the bioactive components in the extract function as capping agents, preventing agglomeration. Prior studies indicate that an increase in extract amount is associated with a decrease in NP agglomeration and size [59].

3.2.3 | Determination the Optimum pH Value

Third, the pH value was adjusted for the production of ZnO NPs. To optimize the pH value, the concentrations of metal salts, the quantity of extract, microwave power, and microwave duration were maintained constant while varying the pH values of 4, 6, 8, 10, and 12. Figure 4 displays absorbance readings obtained from the UV–Vis spectrophotometer within the 300–500 nm

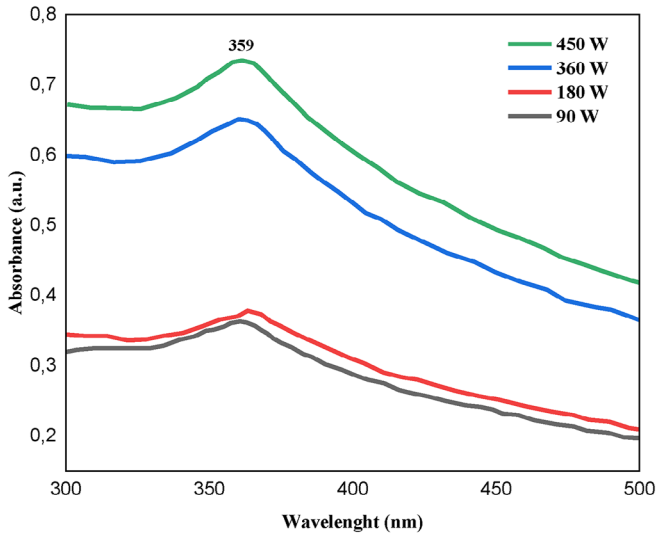

FIGURE 5 | Determination of optimum microwave power.

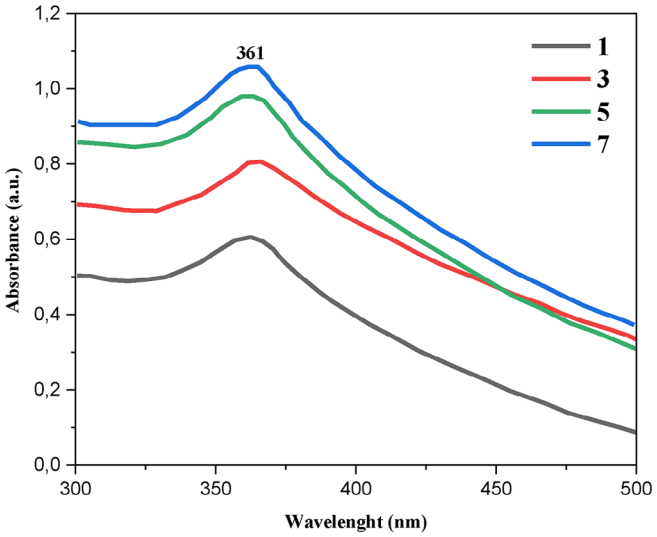

FIGURE 6 | Determination of optimum microwave duration.

wavelength range. No analytical signal was seen between pH 4 and 6; however, a rise in absorbance was noted beginning at pH 8. The peak absorbance was observed at a wavelength of 359 nm at pH 12 conditions. The pH level significantly influences the reduction of metal ions. Changes in the electrical charges of physiologically active compounds link to the influence of pH on synthesis. This impacts their capacity for reduction and capping, thereby influencing the aggregation of NPs [60]. Prior research indicates that an increase in pH value correlates with a reduction in both particle size and aggregation of NPs [61]. Figure 4 illustrates that there was no increase in absorbance in an acidic condition; nevertheless, absorbance began to rise when the condition changed to alkaline. Literature shows that ZnO NPs form in basic and neutral conditions, leading to increasing absorbance at a higher pH [48]. The role of pH in ionization via electron transfer with the metal salt and phytochemicals in the aqueous solution may elucidate this phenomenon, leading to an increase in absorbance and facilitating the creation of ZnO NPs [20].

3.2.4 | Determination of Optimum Microwave Power

The microwave power was tuned for the creation of ZnO NPs. To optimize the synthesis, the concentrations of metal salt, extract volume, pH, and microwave duration were maintained at 90, 180, 360, and 450 W, respectively. Figure 5 displays the absorbance spectra obtained from measurements conducted with the UV–Vis spectrophotometer within the 300–500 nm wavelength range. Analytical signal creation occurred over the characteristic wavelength range at all microwave power levels, with maximum absorbance recorded at 359 nm at 450 W of microwave power. As convection or conduction heats the walls of the reaction vessel, the conventional heating approach requires extended durations for the core of the metal oxide NPs to reach the correct temperature. This results in nonuniform temperature distributions inside the reaction vessel. One way to get around this problem is to use microwave radiation heating, which is between infrared and radio frequencies in the electromagnetic spectrum. This lets the reaction mixture heat up quickly and evenly to the right temperature [62]. Figure 5 illustrates that an increase in microwave power correlates with a rise in absorbance. This scenario is attributed to the rise in microwave power, which elevates the nucleation rate of particles and therefore enhances absorbance due to the production of more NPs. There is evidence from earlier studies that too much microwave power breaks down biologically active parts and makes the NP solution less stable [62, 63]. Consequently, in determining the optimal microwave power, 360 W was selected as the ideal power level, considering ground corrections and maintaining a comparable absorbance value.

3.2.5 | Determination of Optimum Microwave Duration

The microwave duration was optimized for the production of ZnO NPs. To optimize microwave duration, the concentrations of metal salts, extract volume, pH, and microwave power were held constant for 1, 3, 5, and 7 min. Figure 6 presents absorbance measurements acquired from the UV–Vis spectrophotometer in the 300–500 nm wavelength spectrums. Absorbance increases over the typical wavelength range at all time intervals. Peak absorbance accounts for baseline adjustments. The synthesis occurred at 361 nm for a duration of 7 min. As the time of microwave exposure rises, the energy transferred to the system increases proportionally. This indicates that with the passage of time, the reduction of metal salt to ZnO NPs escalates, resulting in an increase in absorbance. Furthermore, prolonged durations were avoided due to concerns that in extended processes, the physiologically active compounds from the extract would undergo hydrolysis, thus diminishing their stabilizing efficacy and leading to agglomeration [63].

3.3 | Characterization of ZnO NPs

3.3.1 | Analysis of UV–Vis Spectroscopy and Band Gap Energy of ZnO NPs

Studies have shown that parameters like concentration, temperature, NP size and shape, and pH influence SPR bands [56]. This work studied and adjusted the variables of pH, extract quantity,

starting salt concentration, microwave power, and microwave duration for the production of ZnO NPs. The optimization process yielded the following ideal conditions: 50 mL of 0.05 M $Zn(NO_3)_2{\cdot}6H_2O$ concentration, 25 mL of extract, pH 12, 360 W of microwave power, and a duration of 7 min. Figure 7a illustrates the UV–Vis absorption spectra of the green-synthesized ZnO NPs. The absorbance peak at around 361 nm strongly shows the presence of ZnO NPs. Gur et al. [64] used a green synthesis method to make ZnO NPs with *Thymbra spicata* L. plant extract and saw a clear absorbance peak at 360 nm. In another work, Abel et al. [65] used coffee leaf extract to synthesize ZnO NPs. The absorption spectra of ZnO NPs exhibited a distinct peak at around 360 nm. This investigation demonstrated that the produced material was ZnO NPs, as shown by the discovery of a comparable peak. The synthesized ZnO NPs were characterized using UV–Vis DRS, and the spectra are shown in Figure 7b. The corresponding band gap value was calculated using the absorption wavelength edge of the NPs obtained from UV–Vis (Figure 7c) [66]. The calculation employed the Kubelka–Munk function for band gap analysis, applying $n = 1/2$ (indirect band gap) for the sample [67]. The determined band gap value was 2.73 eV, which matches what has been reported in the literature about the indirect band gap of ZnO NPs [68].

3.3.2 | XRD Analysis

The XRD technique is used to examine the structure of crystalline metallic NPs. X-rays penetrate the materials being examined and provide insights into their overall structure [7] (Figure 8). The crystallite size (D) of the synthesized ZnO NPs was calculated using the Debye–Scherrer equation [5]:

$$D = \frac{K\lambda}{\beta\cos(\theta)} \tag{5}$$

where D is the crystallite size (nm), K is the shape factor, typically taken as 0.9, λ is the x-ray wavelength (1.5406 A for Cu $K\alpha$), β is the full width at half maximum (FWHM) of the diffraction peak (radians), and θ is the Bragg angle (degrees).

The XRD examination showed that the produced material is ZnO with a wurtzite hexagonal structure, as indexed by JCPDS Card No. 36-1451 [69]. The diffraction peaks at 31.7° (100), 34.4° (002), 36.2° (101), 47.5° (102), 56.6° (110), 62.9° (103), 67.9° (112), 72.5° (004), and 76.9° (202) correspond to the typical planes of ZnO. No impurity phases were observed. The average crystallite size was determined to be 24.46 nm using the Scherrer equation, derived from the peak broadening (FWHM) seen in the XRD pattern (Table 1). The degree of crystallinity was calculated on the basis of the XRD data by evaluating the ratio of crystalline and total areas under the diffraction peaks using the following equation [70]:

$$\%\text{Crystallinity} : \frac{A_{\text{cyristalline}}}{A_{\text{total}}} \times 100 \tag{6}$$

where $A_{\text{cyristalline}}$ represents the area under the crystalline peaks, and A_{total} is the total area under the diffraction pattern, including both crystalline and amorphous regions.

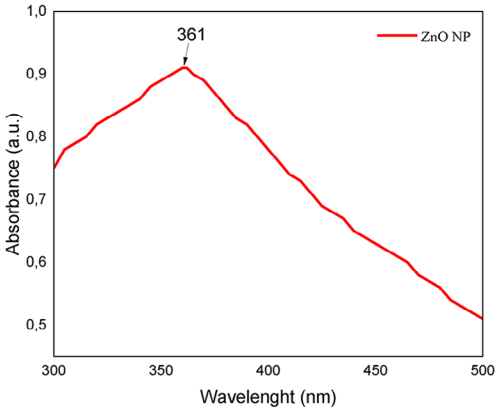

(a)

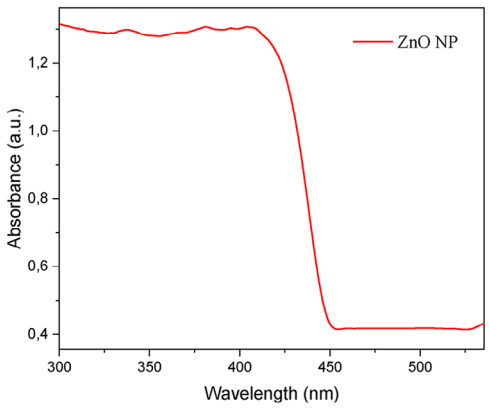

(b)

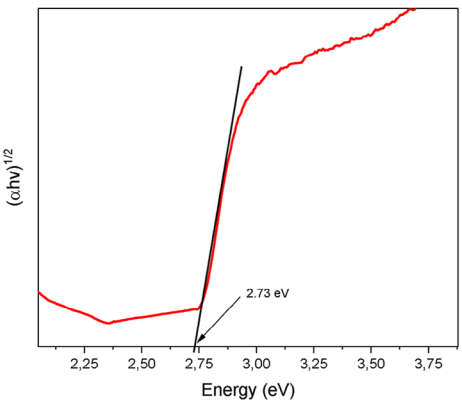

(c)

FIGURE 7 | (a) UV–Visible absorption spectrum of ZnO NPs synthesized under optimum conditions, (b) UV–Visible diffuse reflectance spectra (DRS) of ZnO NPs, (c) Tauc plots of ZnO NPs. ZnO NPs, zinc oxide nanoparticles.

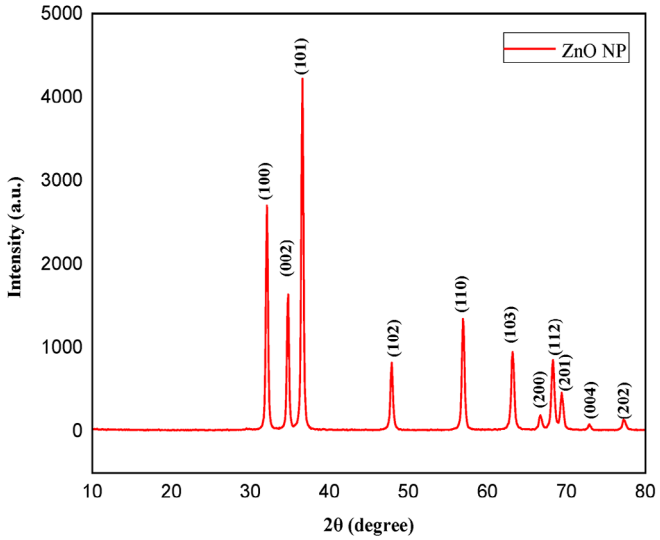

FIGURE 8 | XRD analysis graph of ZnO NPs.

TABLE 1 | The peak values indicate the crystal sizes of ZnO NPs.

2θ (degrees)	FWHM (degrees)	Crystal size (nm)	Miller indices (*h k l*)
32.104	0.298	27.40	100
34.774	0.305	27.294	002
36.593	0.309	27.079	101
47.893	0.348	24.978	102
56.921	0.377	23.969	110
63.202	0.423	22.051	103
66.707	0.452	21.042	200
68.297	0.418	22.965	112
69.409	0.419	23.063	201
72.909	0.361	27.360	004
77.239	0.488	20.836	202
Average		24.460	

Abbreviation: FWHM, full width at half maximum.

In this study, all observed diffraction peaks were assumed to originate solely from the crystalline phase, leading to a calculated crystallinity of 100%.

The percentage porosity was calculated on the basis of the theoretical and bulk densities of the material using the following equation [71]:

$$\%\text{Porosity}: \left(1 - \frac{\rho_{\text{bulk}}}{\rho_{\text{theoritical}}}\right) \times 100 \tag{7}$$

where ρ_{bulk} is the bulk density of the material, which can be determined experimentally, and $\rho_{\text{theoritical}}$ is the theoretical density of ZnO, taken as 5.606 g/cm^3 on the basis of literature.

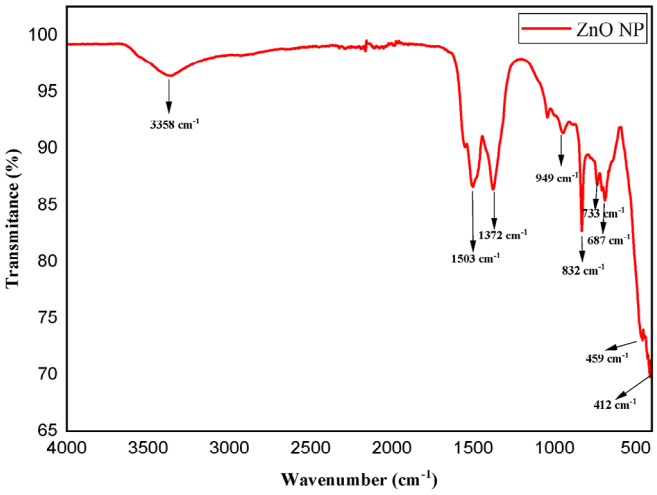

FIGURE 9 | FT-IR analysis graph of ZnO NPs.

The experimental density of ZnO NPs, as determined by XRD data, was 4.82 g/cm^3 [72]. Consequently, porosity was determined to be 14%.

Specific surface area (S) of the material was calculated using the following equation [73]:

$$S: \frac{6}{\rho D} \tag{8}$$

where S is the specific surface area (m^2/g), ρ is the theoretical density of ZnO (5.606 g/cm^3), and D is the average crystallite size (nm), calculated from XRD data using the Scherrer equation.

The produced ZnO NPs exhibited a specific surface area of about 43.706 m^2/g and an average crystallite size of 24.46 nm. This estimate was conducted on the assumption that the particles were spherical and that the density was uniformly distributed throughout the material. The XRD findings correlated with the approaches documented in the current literature [24, 74, 75].

3.3.3 | FT-IR Analysis

The FT-IR study of ZnO NPs produced under optimal conditions is shown in Figure 9. Metal oxides are known to typically exhibit absorption peaks in the 400–600 cm^{-1} range. Therefore, it is known that the vibration tensions between Zn and O atoms are the source of the absorption peaks seen at 459 and 412 cm^{-1} [76, 77]. This result showed the successful synthesis of ZnO NPs. The absorption peak at 3358 cm^{-1} corresponds to O–H stretching [78]. C = C stretching is responsible for the absorption peak at 1503.04 cm^{-1} [79]. A 1372 cm^{-1} corresponds to the bending vibration of C–H bonds [80]. The absorption peaks at 949, 832, 733, and 687 cm^{-1} were attributed to various aromatic functionalities in rosehip seed extract [42]. The results unequivocally demonstrate that the rosehip seed extract is the source of the supplementary peaks in the spectrum, which, aside from the vibrational tensions between Zn and O atoms, confirm the biological coating and stabilization of the ZnO NPs. The results of this study agree with those of earlier research that showed how important functional

TABLE 2 | The dynamic light scattering (DLS) analysis results provide data on particle size (nm) and particle number (%).

Particle size (nm)	Number of particles (%)
36.2	26
42.5	44
47.4	58
51.7	70
55.7	80
59.5	87
63.3	93
67.1	97
71.0	99
75.1	100
79.5	99
84.1	97
89.2	93
94.9	87
101.4	80
109.3	70
119.1	58
132.9	44
156.2	26

groups are in bioreduction of metal salts and stabilization of NPs [56, 82, 83].

3.3.4 | SEM-EDX Analysis

Figure 10a presents an SEM image that illustrates the surface morphology of ZnO NPs, which were synthesized from rosehip seeds using a green synthesis approach. The ZnO NPs have a spherical shape, demonstrate dense aggregation, and show uniform dispersion. In addition, the particle size distribution histogram (Figure 10c) of the SEM images shows that the average size of the ZnO NPs is about 66 nm. Figure 10c illustrates the EDX analysis spectrum used to determine the chemical structure, purity, elemental composition, and stoichiometry of the ZnO NPs. The mass percentage of the synthesized ZnO NPs was 78.20% for zinc and 21.80% for oxygen; the atomic percentage was 46.75% for zinc and 53.25% for oxygen. The SEM-EDX results were corresponded with prior investigations on green synthesis [84, 85].

3.3.5 | DLS Analysis

As shown in Table 2, the DLS method found the size distribution, median diameter (nm), average diameter (nm), and PDI of ZnO NPs made from rosehip seed extract under optimum conditions. The DLS analysis revealed that the NP sizes ranged from 36.2 to 156.2 nm, with a median diameter of 75.1 nm, an average diameter of 82.9 nm, and a PDI value of 0.239. The PDI value,

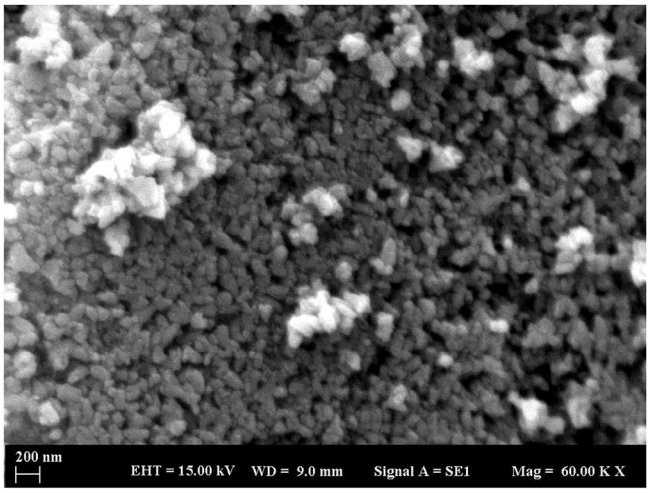

(a)

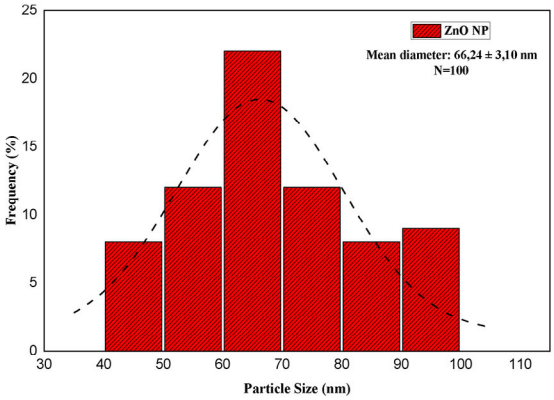

(b)

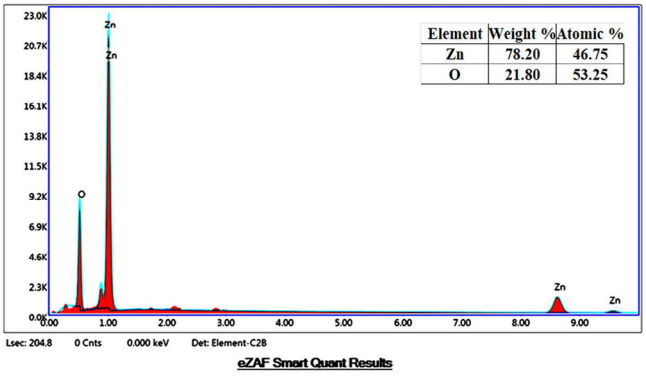

(c)

FIGURE 10 | (a) SEM image, (b) particle size analysis, and (c) EDX spectrum of ZnO NPs.

which quantifies particle size distribution, approaches 0 to signify monodispersity and nears 1 to denote polydispersity [86]. The proximity of the reported PDI value to 0 indicates that the green-produced ZnO NPs possess a monodisperse structure. Furthermore, the average diameter of less than 100 nm suggests the production of ZnO at the nanoscale (Figure 11). Compared to previous green synthesis experiments, the average particle size is

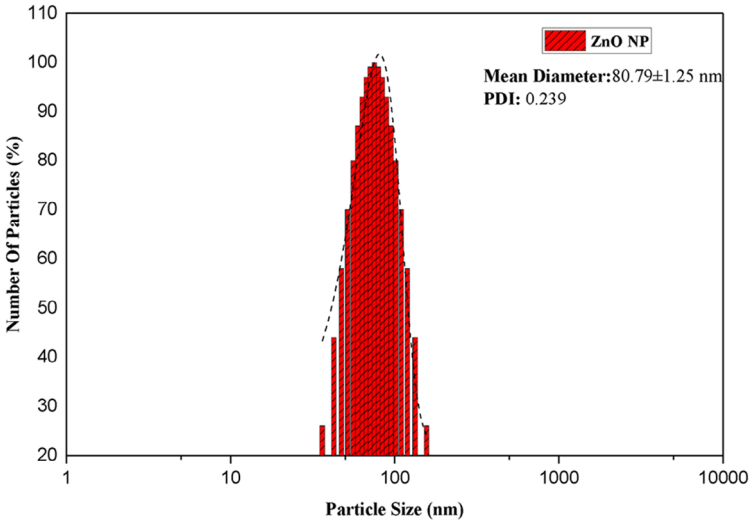

FIGURE 11 | Dynamic light scattering (DLS) analysis of ZnO NPs.

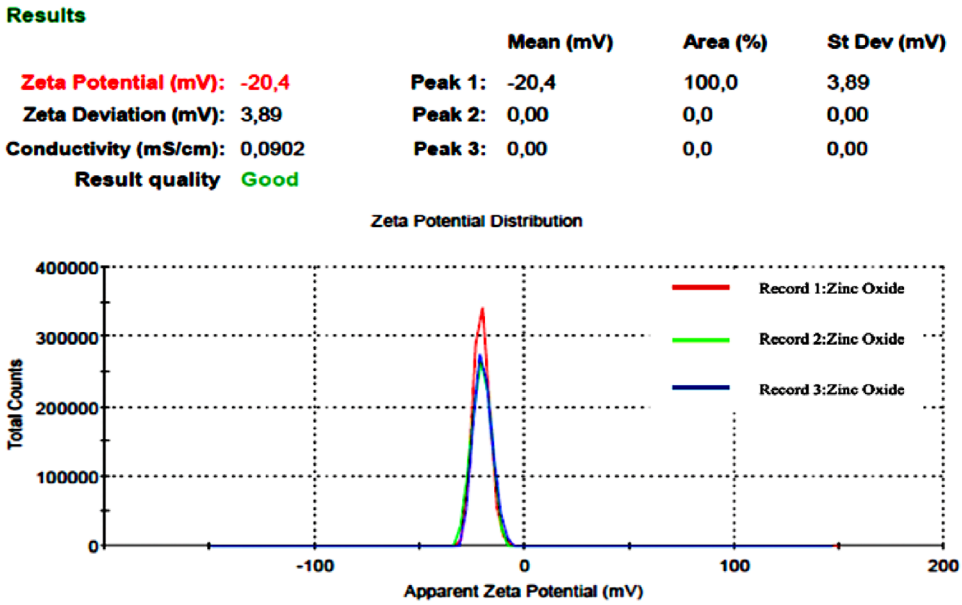

FIGURE 12 | Zeta potential analysis of ZnO NPs.

smaller than most investigations have observed [87, 88]. This is a result of the success of the biologically active components in rosehip seed extract.

3.3.6 | Zeta Potential Analysis

The zeta potential results from the colloidal solution of ZnO NPs made with the green technique and rosehip seed extract are shown in Figure 12. The zeta potential of the NPs was measured at −20.4 ± 3.89 mV. Zeta potential, a measure of the extent of repulsion among charged particles, serves as an indication of their physical stability [89]. Repulsive interparticle interactions inhibit the agglomeration of NPs. It is thought that the reducing agents in rosehip seed extract help make the ZnO NPs, which have a negative charge potential. Furthermore, the negative zeta potential indicates that the produced NPs possess substantial electrostatic forces [77]. Figure 12's result demonstrates the significant stability of the produced NPs [89, 90]. The results align closely with findings reported in previous studies [91, 92].

3.4 | Determination of Phytochemical Content of ZnO NPs

The TPC value of ZnO NPs was determined to be 5.17 ± 0.002 mg GAE/g DM. It is because of their aromatic rings that phenolic compounds and flavonoids can bind to metals and attract nucleophiles. ZnO NPs made by the green approach possess phenolic content. This indicates that phenolic compounds from the plant envelop the NPs, acting as stabilizing and reducing agents [93]. The TFC value was determined to be 120 ± 0.001 mg CE/g DM. The presence of flavonoid content in the produced ZnO NPs is attributed to the role of

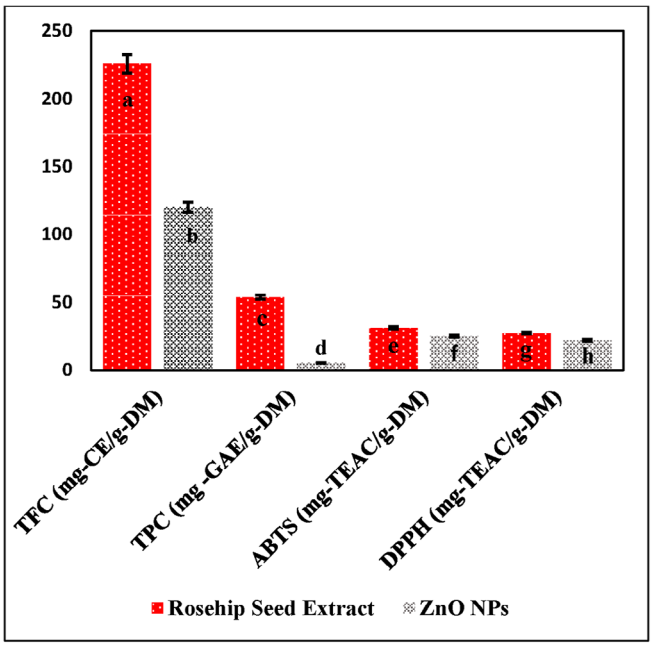

FIGURE 13 | Comparison of TPC, TFC, ABTS, and DPPH findings of rosehip seed extract and ZnO NPs. The data are presented as the mean ($n = 3$) ± standard deviation. Different letters within each column indicate significant differences between treatments according to Tukey's test at $p < 0.001$. ABTS, 2,2′-azinobis(3-ethylbenzothiazoline-6-sulfonic acid); DPPH, 2,2-diphenyl-1-picrylhydrazyl; TFC, total flavonoid content; TPC, total phenolic content; ZnO NPs, zinc oxide nanoparticles.

flavonoid compounds from rosehip seed extract as capping agents for NP stability. The antioxidant activity values of ZnO NPs measured by DPPH and ABTS tests are found to be 21.82 ± 0.004 mg TEAC/g DM and 24.92 ± 0.002 mg TEAC/g DM, respectively. The scavenging effect of ZnO NPs was found to be more than 50% based on the both tests. The TPC and TFC values of ZnO NPs show how well green-produced NPs work as antioxidants. The antioxidant effect of ZnO NPs is due to secondary metabolites made up of flavonoids, which are found in rosehip seeds and have free hydroxyl groups. Consequently, Zn^{2+} is believed to be decreased and stabilized by these secondary metabolites [94]. The research shows variability in the antioxidant properties of ZnO NPs produced using different plant extracts [62, 95, 96]. The NPs, depending on the plant extract and synthesis conditions, exhibit differences in size and surface characteristics. Prior research indicates that NPs have increased radical scavenging activity as their size decreases [95].

Figure 13 displays the antioxidant activity measured by two assays, TPC, and TFC of both rosehip seed extract and zinc ZnO NPs side by side. ZnO NPs exhibit lower TPC, TFC, and antioxidant activity compared to the extract. The findings are found to be statistically different based on $p < 0.001$. Because of the way the compound was made, the phenolic and flavonoid compounds in rosehip seed extract give electrons from their hydroxyl groups to the Zn^{2+} ion. This makes metallic Zn. Metallic zinc is recognized for its reaction with oxygen to produce ZnO NPNPs. The chemicals included in the extract acted as stabilizing agents for the produced ZnO NPs [97]. This suggests that the production of ZnO NPs involves the use of the plant's secondary metabolites. The aforementioned findings suggest that the reduced levels of phenolic and flavonoid chemicals detected in NPs may indicate the involvement of other components present in the plant extract in their creation [93].

4 | Conclusions

The green synthesis method for NP production is eco-friendly and cost-effective. This work successfully produced ZnO NPs using a green technique, which involved the use of rosehip seed *(R. canina* L.) extract. ASE, a sophisticated extraction technique, produced a polyphenol-rich extract. The extract yielded favorable outcomes for TPC, TFC, and antioxidant activity. The microwave heating approach expedited the production of ZnO NPs. The characterization findings showed the production of pure NPs under 100 nm that exhibit antioxidant capabilities. A nanomaterial has been sustainably manufactured using an exceptionally eco-friendly process for diverse applications.

Author Contributions

Rabia Nur Bozkurt: formal analysis, investigation, software, validation. **Selin Şahin**: conceptualization, software, writing–review and editing.

Conflicts of Interest

The authors declare no conflicts of interest.

Ethics Statement

The authors have nothing to report.

Data Availability Statement

The datasets generated during and/or analyzed during the current study are available from the corresponding author on reasonable request.

References

1. V. Kumar, N. K. Kaushik, S. K. Tiwari, D. Singh, and B. Singh, "Green Synthesis of Iron Nanoparticles: Sources and Multifarious Biotechnological Applications," *International Journal of Biological Macromolecules* 253 (2023): 127017.

2. T. Shekofteh Narm, H. Hamidinezhad, Z. Sabouri, and M. Darroudi, "Biosynthesis of Se-Doped $ZnO/Ag_2O/Fe_3O_4$ Nanocomposite Using *Sclerorhachis leptoclada* Extract: Characterization and Investigation of Their Photocatalytic Effects," *Environmental Technology & Innovation* 34 (2024): 103617.

3. A. Selmani, D. Kovačević, and K. Bohinc, "Nanoparticles: From Synthesis to Applications and Beyond," *Advances in Colloid and Interface Science* 303 (2022): 102640.

4. N. Abid, A. M. Khan, S. Shujait, et al., "Synthesis of Nanomaterials Using Various Top-Down and Bottom-Up Approaches, Influencing Factors, Advantages, and Disadvantages: A Review," *Advances in Colloid and Interface Science* 300 (2022): 102597.

5. M. Kermani, A. Mostafapour, Z. Sabouri, S. M. Gheibihayat, and M. Darroudi, "The Photocatalytic, Cytotoxicity, and Antibacterial Properties of Zinc Oxide Nanoparticles Synthesized Using *Trigonella foenum-graecum* L Extract," *Environmental Science and Pollution Research* 30, no. 7 (2023): 19313–19325.

6. Z. Sabouri, M. Kazemi, M. Sabouri, S. S. Tabrizi Hafez Moghaddas, and M. Darroudi, "Biosynthesis of Ag Doped MgO–NiO–ZnO Nanocomposite with *Ocimum basilicum* L Extract and Assessment of Their Biological and Photocatalytic Applications," *Journal of Molecular Structure* 1306 (2024): 137895.

7. D. Titus, E. J. J. Samuel, and S. M. Roopan, *Nanoparticle Characterization Techniques, in Green Synthesis, Characterization and Applications of Nanoparticles* (Amsterdam: Elsevier, 2019), 303–319.

8. N. T. K. Thanh, N. Maclean, and S. Mahiddine, "Mechanisms of Nucleation and Growth of Nanoparticles in Solution," *Chemical Reviews* 114, no. 15 (2014): 7610–7630.

9. N. Genc, I. Yildiz, R. Chaoui, R. Erenler, C. Temiz, and M. Elmastas, "Biosynthesis, Characterization and Antioxidant Activity of Oleuropein-Mediated Silver Nanoparticles," *Inorganic and Nano-Metal Chemistry* 51, no. 3 (2020): 411–419.

10. H. Sonbol, F. Ameen, S. AlYahya, A. Almansob, and S. Alwakeel, "*Padina boryana* Mediated Green Synthesis of Crystalline Palladium Nanoparticles as Potential Nanodrug Against Multidrug Resistant Bacteria and Cancer Cells," *Scientific Reports* 11, no. 1 (2021): 5444.

11. S. C. Mali, A. Dhaka, C. K. Githala, and R. Trivedi, "Green Synthesis of Copper Nanoparticles Using *Celastrus paniculatus* Willd. Leaf Extract and Their Photocatalytic and Antifungal Properties," *Biotechnology Reports* 27 (2020): e00518.

12. H. Mahmood, S. B. Hussain, A. Nosheen, et al., "Antibacterial Activities of Gold Nanoparticles Synthesized by *Citrus limonum* Fruit Extract," *Pakistan Journal of Botany* 53, no. 6 (2021): 2305–2310.

13. K. R. Sumesh and K. Kanthavel, "Green Synthesis of Aluminium Oxide Nanoparticles and Its Applications in Mechanical and Thermal Stability of Hybrid Natural Composites," *Journal of Polymers and the Environment* 27, no. 10 (2019): 2189–2200.

14. J. A. Kumar, T. Krithiga, S. Manigandan, et al., "A Focus to Green Synthesis of Metal/Metal Based Oxide Nanoparticles: Various Mechanisms and Applications Towards Ecological Approach," *Journal of Cleaner Production* 324 (2021): 129198.

15. M. Y. Al-darwesh, S. S. Ibrahim, and M. A. Mohammed, "A Review On Plant Extract Mediated Green Synthesis of Zinc Oxide Nanoparticles and Their Biomedical Applications," *Results in Chemistry* 7 (2024): 101368.

16. M. Martínez-Carmona, Y. Gun'Ko, and M. Vallet-Regí, "ZnO Nanostructures for Drug Delivery and Theranostic Applications," *Nanomaterials* 8, no. 4 (2018): 1–27.

17. Z. Ciğeroğlu, S. Şahin, and E. S. Kazan, "One-Pot Green Preparation of Deep Eutectic Solvent-Assisted ZnO/GO Nanocomposite for Cefixime Trihydrate Photocatalytic Degradation Under UV-A Irradiation," *Biomass Conversion and Biorefinery* 12, no. 1 (2022): 73–86.

18. R. Rathnasamy, P. Thangasamy, R. Thangamuthu, S. Sampath, and V. Alagan, "Green Synthesis of ZnO Nanoparticles Using *Carica papaya* Leaf Extracts for Photocatalytic and Photovoltaic Applications," *Journal of Materials Science: Materials in Electronics* 28, no. 14 (2017): 10374–10381.

19. S. Sadhasivam, M. Shanmugam, P. D. Umamaheswaran, A. Venkattappan, and A. Shanmugam, "Zinc Oxide Nanoparticles: Green Synthesis and Biomedical Applications," *Journal of Cluster Science* 32, no. 6 (2021): 1441–1455.

20. M. Bandeira, M. Giovanela, M. Roesch-Ely, D. M. Devine, and J. da Silva Crespo, "Green Synthesis of Zinc Oxide Nanoparticles: A Review of the Synthesis Methodology and Mechanism of Formation," *Sustainable Chemistry and Pharmacy* 15 (2020): 100223.

21. S. Ying, Z. Guan, P. C. Ofoegbu, et al., "Green Synthesis of Nanoparticles: Current Developments and Limitations," *Environmental Technology & Innovation* 26 (2022): 102336.

22. H. Agarwal, S. Venkat Kumar, and S. Rajeshkumar, "A Review on Green Synthesis of Zinc Oxide Nanoparticles—An Eco-Friendly Approach," *Resource-Efficient Technologies* 3, no. 4 (2017): 406–413.

23. C. Hano and B. H. Abbasi, "Plant-Based Green Synthesis of Nanoparticles: Production, Characterization and Applications," *Biomolecules* 12, no. 1 (2022): 31.

24. R. Hazrati Saadabadi, F. Shariatmadar Tehrani, M. Darroudi, and Z. Sabouri, "Plant-Based Synthesis of ZnO–CeO_2–MgO Nanocomposite Using *Ocimum basilicum* L Seed Extract: Biological Effects and Photocatalytic Activity," *Materials Chemistry and Physics* 314 (2024): 128919.

25. P. K. Dikshit, J. Kumar, A. K. Das, et al., "Green Synthesis of Metallic Nanoparticles: Applications and Limitations," *Catalysts* 11, no. 8 (2021): 902.

26. S. Jadoun, R. Arif, N. K. Jangid, and R. K. Meena, "Green Synthesis of Nanoparticles Using Plant Extracts: A Review," *Environmental Chemistry Letters* 19, no. 1 (2021): 355–374.

27. P. Basnet, T. Inakhunbi Chanu, D. Samanta, and S. Chatterjee, "A Review On Bio-Synthesized Zinc Oxide Nanoparticles Using Plant Extracts as Reductants and Stabilizing Agents," *Journal of Photochemistry and Photobiology B Biology* 183 (2018): 201–221.

28. U. L. Ifeanyichukwu, O. E. Fayemi, and C. N. Ateba, "Green Synthesis of Zinc Oxide Nanoparticles From Pomegranate (*Punica granatum*) Extracts and Characterization of Their Antibacterial Activity," *Molecules (Basel, Switzerland)* 25, no. 19 (2020): 4521.

29. M. N. Alharthi, I. Ismail, S. Bellucci, N. H. Khdary, and A. Salam, "Biosynthesis Microwave-Assisted of Zinc Oxide Nanoparticles With *Ziziphus jujuba* Leaves Extract: Characterization and Photocatalytic Application," *Nanomaterials* 11, no. 7 (2021): 1682.

30. P. Jamdagni, P. Khatri, and J. S. Rana, "Green Synthesis of Zinc Oxide Nanoparticles Using Flower Extract of *Nyctanthes arbor-tristis* and Their Antifungal Activity," *Journal of King Saud University - Science* 30, no. 2 (2018): 168–175.

31. M. MuthuKathija, M. Sheik Muhideen Badhusha, and V. Rama, "Green Synthesis of Zinc Oxide Nanoparticles Using *Pisonia alba* Leaf Extract and Its Antibacterial Activity," *Applied Surface Science Advances* 15 (2023): 100400.

32. J. Du, A. AL-Huqail, Y. Cao, et al., "Green Synthesis of Zinc Oxide Nanoparticles From *Sida acuta* Leaf Extract for Antibacterial and Antioxidant Applications, and Catalytic Degradation of Dye Through the Use of Convolutional Neural Network," *Environmental Research* 258 (2024): 119204.

33. A. Nicolescu, M. Babotă, L. Zhang, et al., "Optimized Ultrasound-Assisted Enzymatic Extraction of Phenolic Compounds From *Rosa canina* L. Pseudo-Fruits (Rosehip) and Their Biological Activity," *Antioxidants* 11 , no. 6 (2022): 1123.

34. Y. Mourabit, S. El Hajjaji, D. Taha, et al., "HPLC-DAD-ESI/MS Phytochemical Investigation, Antioxidant, and Antidiabetic Activities of Moroccan *Rosa canina* L. Extracts," *Biocatalysis and Agricultural Biotechnology* 52 (2023): 102817.

35. D. Paunović, A. Kalušević, T. Petrović, et al., "Assessment of Chemical and Antioxidant Properties of Fresh and Dried Rosehip (*Rosa canina* L)," *Notulae Botanicae Horti Agrobotanici Cluj-Napoca* 47, no. 1 (2019): 108–113.

36. H. Ilyasoğlu, "Characterization of Rosehip (*Rosa canina* L.) Seed and Seed Oil," *International Journal of Food Properties* 17, no. 7 (2014): 1591–1598.

37. M. Güney, "Determination of Fatty Acid Profile and Antioxidant Activity of Rosehip Seeds From Turkey," *International Journal of Agriculture, Environment and Food Sciences* 4, no. 1 (2020): 114–118.

38. J. Popović-Djordjević, B. Špirović-Trifunović, I. Pećinar, et al., "Fatty Acids in Seed Oil of Wild and Cultivated Rosehip (*Rosa canina* L.) From Different Locations in Serbia," *Industrial Crops and Products* 191 (2023): 115797.

39. K. Ozlem Saygi and C. Usta, "*Rosa canina* Waste Seed Extract-Mediated Synthesis of Silver Nanoparticles and the Evaluation of Its Antimutagenic Action in *Salmonella typhimurium*," *Materials Chemistry and Physics* 266 (2021): 124537.

40. J. Švarc-Gajić and S. Morais, "Recent Advances in the Development and Application of Green Extraction Techniques," *Applied Sciences* no. 20 (2022): 12.

41. H. Sun, X. Ge, Y. Lv, and A. Wang, "Application of Accelerated Solvent Extraction in the Analysis of Organic Contaminants, Bioactive and Nutritional Compounds in Food and Feed," *Journal of Chromatography A* 1237 (2012): 1–23.

42. M. Repajić, E. Cegledi, V. Kruk, et al., "Accelerated Solvent Extraction as a Green Tool for the Recovery of Polyphenols and Pigments From Wild Nettle Leaves," *Processes* 8, no. 7 (2020): 803.

43. A. Vilas-Franquesa, B. Juan, and J. Saldo, "Targeted Analysis of Sea Buckthorn Oil Extracted by Accelerated Solvent Extraction Technique Using Green and Conventional Solvents," *LWT* 164 (2022): 113643.

44. D. T. Ayele, M. L. Akele, and A. T. Melese, "Analysis of Total Phenolic Contents, Flavonoids, Antioxidant and Antibacterial Activities of Croton *m*acrostachyus Root Extracts," *BMC Chemistry* 16 no. 1 (2022): 65.

45. A. M. Shraim, T. A. Ahmed, M. M. Rahman, and Y. M. Hijji, "Determination of Total Flavonoid Content by Aluminum Chloride Assay: A Critical Evaluation," *LWT* 150 (2021): 111932.

46. S. Baliyan, R. Mukherjee, A. Priyadarshini, et al., "Determination of Antioxidants by DPPH Radical Scavenging Activity and Quantitative Phytochemical Analysis of *Ficus religiosa*," *Molecules (Basel, Switzerland)* 27 no. 4 (2022): 1176.

47. S. Şahin, "A Novel Technology for Extraction of Phenolic Antioxidants from Mandarin (*Citrus deliciosa* Tenore) Leaves: Solvent-Free Microwave Extraction," *Korean Journal of Chemical Engineering* 32 (2015): 950–957.

48. F. A. M. Alahdal, M. T. A. Qashqoosh, Y. K. Manea, M. A. S. Salem, A. M. T. Khan, and S. Naqvi, "Eco-Friendly Synthesis of Zinc Oxide Nanoparticles as Nanosensor, Nanocatalyst and Antioxidant Agent Using Leaf Extract of *P. austroarabica*," *Austroarabica OpenNano* 8 (2022): 100067.

49. G. Spigno, L. Tramelli, and D. M. De Faveri, "Effects of Extraction Time, Temperature and Solvent on Concentration and Antioxidant Activity of Grape Marc Phenolics," *Journal of Food Engineering* 81, no. 1 (2007): 200–208.

50. J. R. Mufari, A. C. Rodríguez-Ruiz, A. E. Bergesse, P. P. Miranda-Villa, V. Nepote, and A. R. Velez, "Bioactive Compounds Extraction From Malted Quinoa Using Water–Ethanol Mixtures Under Subcritical Conditions," *LWT* 138 (2021): 110574.

51. J. Mitrović, N. Nikolić, I. Karabegović, et al., "Evaluation of the Solvent Effect on the Extraction and Antioxidant Activity of Phenolic Compounds From the Nettle (*Urtica dioica* L.) Seeds: Application of PCA and Regression Analyses," *Journal of Food Measurement and Characterization* 18, no. 11 (2024): 6618–6626.

52. M. Doulabi, M. T. Golmakani, and S. Ansari, "Evaluation and Optimization of Microwave-Assisted Extraction of Bioactive Compounds From Eggplant Peel By-Product," *Journal of Food Processing and Preservation* 44, no. 11 (2020): e14853.

53. N. Demir, O. Yildiz, M. Alpaslan, and A. A. Hayaloglu, "Evaluation of Volatiles, Phenolic Compounds and Antioxidant Activities of Rose Hip (*Rosa* L.) Fruits in Turkey," *LWT—Food Science and Technology* 57, no. 1 (2014): 126–133.

54. F. Demir and M. Özcan, "Chemical and Technological Properties of Rose (*Rosa canina* L.) Fruits Grown Wild in Turkey," *Journal of Food Engineering* 47, no. 4 (2001): 333–336.

55. N. B. Gaber, S. I. El-Dahy, and E. A. Shalaby, "Comparison of ABTS, DPPH, Permanganate, and Methylene Blue Assays for Determining Antioxidant Potential of Successive Extracts From Pomegranate and Guava Residues," *Biomass Conversion and Biorefinery* 11, no. 5 (2021): 4011–4020.

56. M. Gupta, R. S. Tomar, S. Kaushik, R. K. Mishra, and D. Sharma, "Effective Antimicrobial Activity of Green ZnO Nano Particles of *Catharanthus roseus*," *Frontiers in Microbiology* 9 (2018): 2030.

57. F. H. Abdullah, N. H. H. Abu Bakar, and M. Abu Bakar, "Low Temperature Biosynthesis of Crystalline Zinc Oxide Nanoparticles From *Musa acuminata* Peel Extract for Visible-Light Degradation of Methylene Blue," *Optik (Stuttg)* 206 (2020): 164279.

58. M. R. Dar, A. K. Khan, M. Inam, C. Hano, and S. Anjum, "Differential Impact of Zinc Salt Precursors on Physiognomies, Anticancerous, and Antibacterial Activities of Zinc Oxide Nanoparticles," *Applied Biochemistry and Biotechnology* 196, no. 8 (2024): 4874–4899.

59. M. M. H. Khalil, E. H. Ismail, K. Z. El-Baghdady, and D. Mohamed, "Green Synthesis of Silver Nanoparticles Using Olive Leaf Extract and Its Antibacterial Activity," *Arabian Journal of Chemistry* 7, no. 6 (2014): 1131–1139.

60. H. Padalia, S. Baluja, and S. Chanda, "Effect of pH on Size and Antibacterial Activity of *Salvadora oleoides* Leaf Extract-Mediated Synthesis of Zinc Oxide Nanoparticles," *Bionanoscience* 7, no. 1 (2017): 40–49.

61. X. Wang, T. Sun, H. Zhu, T. Han, J. Wang, and H. Dai, "Roles of pH, Cation Valence, and Ionic Strength in the Stability and Aggregation Behavior of Zinc Oxide Nanoparticles," *Journal of Environmental Management* 267 (2020): 110656.

62. S. Jafarirad, M. Mehrabi, B. Divband, and M. Kosari-Nasab, "Biofabrication of Zinc Oxide Nanoparticles Using Fruit Extract of *Rosa canina* and Their Toxic Potential Against Bacteria: A Mechanistic Approach," *Materials Science and Engineering C* 59 (2016): 296–302.

63. O. Długosz and M. Banach, "Continuous Synthesis of Metal and Metal Oxide Nanoparticles in Microwave Reactor," *Colloids and Surfaces A: Physicochemical and Engineering Aspects* 606 (2020): 125453.

64. T. Gur, I. Meydan, H. Seckin, M. Bekmezci, and F. Sen, "Green Synthesis, Characterization and Bioactivity of Biogenic Zinc Oxide Nanoparticles," *Environmental Research* 204 (2022): 111897.

65. S. Abel, J. L. Tesfaye, R. Shanmugam, et al., "Green Synthesis and Characterizations of Zinc Oxide (ZnO) Nanoparticles Using Aqueous Leaf Extracts of Coffee (*Coffea arabica*) and Its Application in Environmental Toxicity Reduction," *Journal of Nanomaterials* 2021, no. 1 (2021): 3413350.

66. İ. Kaba and Ö. Kerkez-Kuyumcu, "Optimization of the Boosted Photocatalytic H_2 Production by Rationally Designated $Cd_xZn_{1-x}S/MoS_2$," *International Journal of Green Energy* 21, no. 6 (2024): 3675–3685.

67. S. Yılmaz, Ö. K. Kuyumcu, Ş. S. Bayazit, R. M. Z. Ayaz, D. Akyüz, and A. Koca, "Enhanced Photoelectrochemical Activity of Magnetically Modified TiO_2 Prepared by a Simple Ex-Situ Route," *Journal of Solid State Electrochemistry* 26 (2022): 245–255.

68. L. M. Peddada, S. R. Sagurthi, V. C. Guguloth, R. Annapragada, and P. R. Kanuparthy, "Visible Light Driven Photodegradation of Pathological Effluents and Biological Evaluation of Green ZnO Nanoparticles," *ChemistrySelect* 7, no. 28 (2022): e202200146.

69. N. Sedefoglu, "Green Synthesis of ZnO Nanoparticles by *Myrtus communis* Plant Extract With Investigation of Effect of Precursor, Calcination Temperature and Study of Photocatalytic Performance," *Ceramics International* 50, no. 6 (2024): 9884–9895.

70. A. A. Barzinjy and H. H. Azeez, "Green Synthesis and Characterization of Zinc Oxide Nanoparticles Using *Eucalyptus globulus* Labill. Leaf Extract And Zinc Nitrate Hexahydrate Salt," *SN Applied Sciences* 2, no. 5, (2020): 991.

71. S. Saleem, M. H. Jameel, A. Rehman, et al., "Evaluation of Structural, Morphological, Optical, and Electrical Properties of Zinc Oxide Semiconductor Nanoparticles With Microwave Plasma Treatment for Electronic

Device Applications," *Journal of Materials Research and Technology* 19, (2022): 2126–2134.

72. A. Khorsand Zak, W. H. Abd. Majid, M. E. Abrishami, and R. Yousefi, "X-Ray Analysis of ZnO Nanoparticles by Williamson–Hall and Size–Strain Plot Methods," *Solid State Sciences* 13, no. 1 (2011): 251–256.

73. C. Chen, P. Liu, and C. Lu, "Synthesis and Characterization of Nano-Sized ZnO Powders by Direct Precipitation Method," *Chemical Engineering Journal* 144, no. 3 (2008): 509–513.

74. L. Tabassam, M. J. Khan, S. Hussain, S. A. Khattak, S. K. Shah, and A. S. Bhatti, "Structural, Optical and Antimicrobial Characteristics of ZnO Green Nanoparticles," *Journal of Sol-Gel Science and Technology* 101, no. 2, (2022): 401–410.

75. M. M. Chikkanna, S. E. Neelagund, and K. K. Rajashekarappa, "Green Synthesis of Zinc Oxide Nanoparticles (ZnO NPs) and Their Biological Activity," *SN Applied Sciences* 1, no. 1 (2019): 1–10.

76. S. Fakhari, M. Jamzad, and H. Kabiri Fard, "Green Synthesis of Zinc Oxide Nanoparticles: A Comparison," *Green Chemistry Letters and Reviews* 12, no. 1 (2019): 19–24.

77. A. S. Abdelbaky, T. A. Abd El-Mageed, A. O. Babalghith, S. Selim, and A. M. H. A. Mohamed, "Green Synthesis and Characterization of ZnO Nanoparticles Using *Pelargonium odoratissimum* (L.) Aqueous Leaf Extract and Their Antioxidant," *Antibacterial and Anti-inflammatory Activities Antioxidants* 11, no. 8 (2022): 1444.

78. M. Mohammadian, Z. Es'haghi, and S. Hooshmand, "Green and Chemical Synthesis of Zinc Oxide Nanoparticles and Size Evaluation by UV–Vis Spectroscopy," *Nanomedicine Research Journal* 7, no. 1, (2018): 00175.

79. S. Ravichandran, J. Radhakrishnan, P. Sengodan, R. Rajendran, R. Ramalingam, and K. D. Arunachalam, "Bio Synthesis of Zinc Oxide Nanoparticles Using *Clerodendrum phlomidis* Extract for Antibacterial, Anticancer, Antioxidant and Photocatalytic Studies," *Journal of Materials Science: Materials in Electronics* 33, no. 14, (2022): 11455–11466.

80. K. Nagaraja, M. Arunpandian, and O. H. Tae Hwan, "Facile Bio-Inspired Synthesis of Polysaccharide-Mediated Zinc Oxide Nanoparticles and Their Efficient Antimicrobial and Photocatalytic Activity," *Colloids and Surfaces A: Physicochemical and Engineering Aspects* 688, (2024): 133564.

81. M. Ganesh, S. G. Lee, J. Jayaprakash, M. Mohankumar, and H. T. Jang, "*Hydnocarpus alpina* Wt Extract Mediated Green Synthesis of ZnO Nanoparticle and Screening of Its Anti-Microbial, Free Radical Scavenging, and Photocatalytic Activity," *Biocatalysis and Agricultural Biotechnology* 19, (2019): 101129.

82. S. Gunalan, R. Sivaraj, and V. Rajendran, "Green Synthesized ZnO Nanoparticles against Bacterial and Fungal Pathogens," *Progress in Natural Science: Materials International* 22, no. 6 (2012): 693–700.

83. M. Anbuvannan, M. Ramesh, G. Viruthagiri, N. Shanmugam, and N. Kannadasan, "Synthesis, Characterization and Photocatalytic Activity of ZnO Nanoparticles Prepared by Biological Method," *Spectrochimica Acta Part A, Molecular and Biomolecular Spectroscopy* 143 (2015): 304–308.

84. K. Elumalai and S. Velmurugan, "Green Synthesis, Characterization and Antimicrobial Activities of Zinc Oxide Nanoparticles From the Leaf Extract of *Azadirachta indica* (L.)," *Applied Surface Science* 345 (2015): 329–336.

85. S. Vijayakumar, S. Mahadevan, P. Arulmozhi, S. Sriram, and P. K. Praseetha, "Green Synthesis of Zinc Oxide Nanoparticles Using *Atalantia monophylla* Leaf Extracts: Characterization and Antimicrobial Analysis," *Materials Science in Semiconductor Processing* 82, (2018): 39–45.

86. O. M. Elshayb, K. Y. Farroh, H. E. Amin, and A. M. Atta, "Green Synthesis of Zinc Oxide Nanoparticles: Fortification for Rice Grain Yield and Nutrients Uptake Enhancement," *Molecules (Basel, Switzerland)* 26, no. 3 (2021): 584.

87. H. M. Abdelmigid, N. A. Hussien, A. A. Alyamani, M. M. Morsi, N. M. AlSufyani, and H. A. Kadi, "Green Synthesis of Zinc Oxide Nanoparticles Using Pomegranate Fruit Peel and Solid Coffee Grounds vs. Chemical Method of Synthesis, With Their Biocompatibility and Antibacterial Properties Investigation," *Molecules (Basel, Switzerland)* 27, no. 4 (2022): 1236.

88. A. Can and K. Kızılbey, "Green Synthesis of ZnO Nanoparticles via *Ganoderma lucidum* Extract: Structural and Functional Analysis in Polymer Composites," *Gels* 9 (2024): 10.

89. R. Shah, D. Eldridge, E. Palombo, and I. Harding, "Optimisation and Stability Assessment of Solid Lipid Nanoparticles Using Particle Size and Zeta Potential," *Journal of Physical Science* 25, no. 1 (2014): 59–75.

90. C. Cano-Sarmiento, D. I. Téllez-Medina, R. Viveros-Contreras, et al., *Zeta Potential of Food Matrices Food Engineering Reviews* 10, no. 3, (2018): 113–138.

91. A. Q. Nkemzi, K. Okaiyeto, O. Oyenihi, C. S. Opuwari, O. E. Ekpo, and O. O. Oguntibeju, "Antidiabetic, Anti-Inflammatory, Antioxidant, and Cytotoxicity Potentials of Green-Synthesized Zinc Oxide Nanoparticles Using the Aqueous Extract of *Helichrysum cymosum*," *3 BioTechniques* 14, no. 12 (2024): 291.

92. D. A. Hamdy, M. A. M. Ismail, H. M. El-Askary, et al., "Green Synthesis of Zinc Oxide/*Allium sativum* Nano-Composite and Its Efficacy Against Murine Cryptosporidiosis," *Microscopy Research and Technique* 87, no. 1 (2024): 3–15.

93. A.-R. Phull, Q. Abbas, A. Ali, et al., "Antioxidant, Cytotoxic and Antimicrobial Activities of Green Synthesized Silver Nanoparticles From Crude Extract of *Bergenia ciliata*," *Future Journal of Pharmaceutical Sciences* 2, no. 1 (2016): 31–36.

94. M. Alavi, N. Karimi, and I. Salimikia, "Phytosynthesis of Zinc Oxide Nanoparticles and Its Antibacterial, Antiquorum Sensing, Antimotility, and Antioxidant Capacities Against Multidrug Resistant Bacteria," *Journal of Industrial and Engineering Chemistry* 72 (2019): 457–473.

95. M. Stan, A. Popa, D. Toloman, T. D. Silipas, and D. C. Vodnar, "Antibacterial and Antioxidant Activities of ZnO Nanoparticles Synthesized Using Extracts of *Allium sativum*, *Rosmarinus officinalis* and *Ocimum basilicum*," *Acta Metallurgica Sinica (English Letters)* 29, no. 3 (2016): 228–236.

96. Y. Gao, M. Arokia Vijaya Anand, V. Ramachandran, et al., "Biofabrication of Zinc Oxide Nanoparticles From *Aspergillus niger*, Their Antioxidant, Antimicrobial and Anticancer Activity," *Journal of Cluster Science* 30, no. 4 (2019): 937–946.

97. A. Klinbumrung, R. Panya, A. Pung-Ngama, P. Nasomjai, J. Saowalakmeka, and R. Sirirak, "Green Synthesis of ZnO Nanoparticles by Pineapple Peel Extract From Various Alkali Sources," *Journal of Asian Ceramic Societies* 10, no. 4 (2022): 755–765.